

Article

Not peer-reviewed version

Comparison of Cerium Nanoparticles Toxicity against *Bacillus subtilis* Grown in Two Different Types of Biofilm

[Elisabeth Darrouzet](#)^{*}, [Sylvie Luche](#), H  l  ne Diemer, [Sarah Cianf  rani](#), [Thierry Rabilloud](#), [C  cile Lelong](#)^{*}

Posted Date: 5 September 2024

doi: 10.20944/preprints202409.0448.v1

Keywords: *Bacillus subtilis*; biofilm; swarming; proteomics; cerium oxide nanoparticles; silica nanoparticles



Preprints.org is a free multidiscipline platform providing preprint service that is dedicated to making early versions of research outputs permanently available and citable. Preprints posted at Preprints.org appear in Web of Science, Crossref, Google Scholar, Scilit, Europe PMC.

Copyright: This is an open access article distributed under the Creative Commons Attribution License which permits unrestricted use, distribution, and reproduction in any medium, provided the original work is properly cited.

pathways affected by the toxicants and propose mechanistic models. In this way, prediction of agonist/antagonist action of various pollutants could be feasible. However, for this, appropriate growth conditions should be selected.

Bacillus subtilis is an essential component of the rhizosphere and some species can colonize the gastrointestinal tracts of different animal species including human. It is also used as feeding for broiler chickens or fish to improve growth performance, as vaccine carrier in animal health or as a probiotic, including for humans [1]. The genome of this soil model bacterium is sequenced and many experimental data concerning its metabolism, protein function, regulons... are available including a dedicated database (Subtiwiki) [2], which is very useful to interpret the information resulting from OMICs analyses. *B. subtilis* can grow as planktonic cells in aquatic environment (fresh water) but in its natural ecosystem, this bacterium develops mainly in the form of a biofilm, particularly around plant roots. For facility reasons many studies are focused on liquid agitated cultures but biofilm mode of growth is much closer to its natural environment and to the mode of growth of many soil bacteria, including those growing in the biofilm matrix produced by other bacteria. *B. subtilis* has several life styles including pellicle biofilm and swarming. Contrary to planktonic cells, in these two modes, cells are growing in communities and are differentiated, forming highly complex structures [3,4]. A static culture in liquid favors the formation of a pellicle biofilm at the air water interface whereas culture on soft agar promotes swarming (fast mode of bacterial translocation) and with time the formation of a sort of macro-colony/biofilm. Noteworthy, some strains of *B. subtilis* are also able to form immersed biofilms [5]. For root colonizing for example, both swarming and biofilm with sessile cells are required [6]. Many studies relying on biochemistry, molecular biology or even biophysical technics have been performed to understand these two life-styles [7,8]. Pisithkul et al. have even performed a well documented study (metabolomics, transcriptomics and proteomics) to analyse biofilm formation [9], but to the best of our knowledge, no study has used proteomics to have a whole proteome view of the modulated pathways between swarming and pellicle biofilm.

Even if most studies deal with nanoparticles (NPs) toxicity on animal cells that can internalize the particles (endocytosis, phagocytosis), some studies have already been performed on bacteria especially in respect to NP bactericidal effect [10–12]. However, more and more NPs are encountered in the environment that are not there purposely for their bactericidal effect but rather as pollutants resulting from human activities. Indeed, more and more NPs are used for example for coating fabrics (stain-repellent), walls (anti-graffiti, crack resistant paints), windows (self-cleaning) and solar cells, or incorporated in personal care product including sunscreens. Nanoceria (Ce oxide NPs) is one of these expanding nanomaterials with antibacterial action but also widely used for example as polishing agent, in ultraviolet absorbers and as an additive in fuels in order to improve combustion. Nanosilica is a strong abrasive material also used for polishing and has capacity to reduce friction. Several studies have looked especially at cerium (Ce) or silicon (Si) oxide NP toxicity in term of bactericidal action by disk diffusion or growth inhibition methods [13–15]. Krishnamoorthy et al. studied Ce oxide nanocubes toxicity and showed an impact on membrane integrity in agitated liquid culture. At last, Pelletier et al. have studied the effect of nanoceria particles on the growth and viability of gram+ and gram- bacteria, including a transcriptomic analysis on *Escherichia coli*, and examined the influence of nanoceria size, pH and type of growth media on *B. subtilis* [16]. Contrary to other metallic NPs, Ce oxide is supposed to have antioxidant properties and is used as such in medicine to alleviate oxidative stress linked diseases. However, this effect seems to be much more complex, depending on the pH and on particle coating including that resulting from molecules present in the culture medium [17].

We used the power of shotgun proteomics and bioinformatics tools to analyze in details the complexity and adaptability of *B. subtilis* proteome in two somehow similar modes of cultures: swarming and pellicle biofilm. Several physiological and metabolic patterns including proteins implicated in sporulation have shown significant differences triggered by the growth culture modes.

Then, instead of testing the influence of NP size, medium, pH..., as other studies did, we studied in the same way by comparative proteomics the influence of these two growing modes on the effect of nanosilica and nanoceria. We focused on nanoceria and showed that these particles do not trigger

the same changes in term of stringent response, sporulation or even iron homeostasis between the different culture modes. This clearly highlights the importance of eventually testing several growth conditions and pinpoints the power of proteomics to decipher subtle changes at the whole proteome level.

2. Materials and Methods

2.1. Bacterial Strain Culture Media and Chemicals

The *B. subtilis* strain used was the NCIB3610 strain (wild type) (from the Bacillus Genetic Stock Center, BGSCID 3A1). The medium was Luria-Bertani (LB): 10 g/L tryptone, 5 g/L yeast extract and 5 g/L NaCl. The NPs were from SIGMA: n-CeO₂, reference 643009 and amorphous SiO₂, reference S5505. They were purchased as soluble dispersions.

2.2. DLS Measurements

Just before measurements with the dynamic light scattering device (DLS, Wyatt technology), nanoparticles were diluted into three different solutions (H₂O, LB medium or preconditioned LB medium). The preconditioned LB was prepared as follows: *Bacillus subtilis* strain 3610 was grown in LB until an OD_{600 nm} of 0.6. Then, 2 ml of culture was harvested by centrifugation at 13,000 rpm for 10 min. The supernatant was filtered through a 0.2 µm filter. The filtered solution constituted preconditioned LB. All the solutions (H₂O, LB medium or preconditioned LB medium) were filtered before addition of the nanoparticles. Each measurement was performed at least in triplicate.

2.3. Growth Conditions

B. subtilis was first grown overnight at 37°C in Luria-Bertani (LB) in Erlenmeyer flasks with shaking at 200 rpm.

For the swarming mode, growth on soft solid agar LB medium was performed using a six-well plate. Each well was filled with 7 mL of LB agar (10g/L agar in LB) containing or not Ce or Si oxide NPs at a concentration of 10 µg/mL (Ce^{II} or Si^{II}) or 0.1 µg/mL (Ce^I or Si^I). The multi-well plates were dried overnight (15h) at 37°C before being used. A 3610 *B. subtilis* overnight culture was diluted to A_{600 nm}= 0.1 in 10 mL of fresh LB medium and incubated at 37°C and 200 rpm until the A_{600 nm} reached 0.7. 3 µL of this culture were inoculated in the middle of each well. The plates were then incubated at 30°C for 48h. All the cells contained in a well were recovered using a sterile plastic öse, directly put in sterile microtube and quickly frozen at -20°C.

For the pellicle biofilm growth mode, A 3610 *B. subtilis* overnight culture was diluted to A_{600nm}= 0.04 in fresh LB medium containing or not NPs. 4 mL per well of the liquid bacterial solution was aliquoted in the six-well plate which was then incubated without shaking at 30°C for 48h. After carefully removing the planktonic bacteria, the sessile bacteria forming a pellicle biofilm were resuspended in 1 ml of PBS and rinsed twice in PBS before being frozen.

For mass spectrometry, experiments were performed in quadruplicate (four independent cultures).

2.4. Protein Extraction and Quantification

The bacterial pellets were extracted with 100 µL of lysis solution (4 M urea, 2.5% CTAC (cetyl trimethyl ammonium chloride), 100 mM phosphate buffer pH 3 and methylene blue 150 µM) as in [18,19]. After extraction at room temperature for 30 minutes, the extracts were clarified by centrifugation (15,000 g 15 min), the supernatants collected and their protein concentration determined by a modified Bradford assay containing α-cyclodextrin [20]. Protein extracts were stored frozen at -20 °C until use.

2.5. Shotgun Analysis

2.5.1. Sample Preparation

For shotgun proteomic analyses, the samples were included in polyacrylamide plugs using the photopolymerization system described in Muller et al. 2018, and Lyubimova et al. 1993 [19,21].

When needed, samples were diluted in the CTAC buffer to obtain a concentration of 8, 6 and 4.5 µg per 15 µL for all swarming, pellicle biofilm 48h and pellicle biofilm 72h samples, respectively. The initiator solutions consisted in a 1 M solution of sodium toluene sulfinate in water and in a saturated water solution of diphenyliodonium chloride. The ready-to-use polyacrylamide solution consisted of 1 mL of a commercial 40% acrylamide/bis solution (37.5/1) to which 100 µL of diphenyliodonium chloride solution, 100 µL of sodium toluene sulfinate solution and 300 µL of water were added.

5 µL of acrylamide solution were added to the 15 µL of protein samples already containing the methylene dye and 100 µL of water-saturated butanol were then layered on top of the samples. Polymerization was carried out for 2 h under a 1500 lm 2700 K LED lamp. At the end of the polymerization period, the butanol was removed, the gel plugs transferred in a 96 well plate and fixed for 1 hr with 20% ethanol, 5% phosphoric acid, followed by a 3*15 min washes in 30% ethanol. The fixed gel plugs were then stored at -20 °C until use.

The gel plugs were washed three times with 50 µL of 25 mM ammonium hydrogen carbonate (NH₄HCO₃) and 50 µL of acetonitrile. The cysteine residues were reduced by 50 µL of 10 mM dithiothreitol at 57°C for 45 min and alkylated by 50 µL of 55 mM iodoacetamide for 30 min. After two washes with NH₄HCO₃ and acetonitrile, the gel plugs were dehydrated by acetonitrile. The digestion of proteins was done in gel with 20 µL of 12 ng/µL of modified porcine trypsin (Promega, Madison, WI, USA) in 25 mM NH₄HCO₃. The digestion was performed overnight at room temperature. The generated peptides were extracted with 50 µL of 60% acetonitrile in 0.1% formic acid. Acetonitrile was evaporated under vacuum and samples were resuspended with 20 µL of a solution containing 2% acetonitrile and 0.1% formic acid.

2.5.2. Mass Spectrometry Analysis

NanoLC-MS/MS analysis was performed using a nanoACQUITY Ultra-Performance-LC (Waters Corporation, Milford, USA) coupled to a Q-Exactive Plus mass spectrometer (Thermo Fisher Scientific, Bremen, Germany). The complete system was fully controlled by Thermo Scientific™ Xcalibur™ software (v3.1).

Samples (640 ng) were first concentrated/desalted onto a NanoEase™ M/Z Symmetry C18 precolumn (100Å, 5 µm, 180 µm × 20 mm, Waters Corporation, Milford, USA) using 99% of solvent A (0.1% formic acid in water) and 1% of solvent B (0.1% formic acid in acetonitrile) at a flow rate of 5 µL/min for 3 min. A solvent gradient from 1 to 8% of B in 2 min then from 8 to 35% of B in 77 min was used for peptide elution, which was performed at a flow rate of 400 nL/min using a NanoEase™ M/Z BEH C18 column (130Å, 1.7 µm, 75 µm × 250 mm, Waters Corporation, Milford, USA) maintained at 60 °C.

The Q-Exactive Plus was operated and MS parameters set as described in Quque et al. 2023 [22]. Raw data were converted into mgf files using the MSConvert tool from ProteomeWizard (v3.0.6090; <http://proteowizard.sourceforge.net/>).

2.5.3. Protein Identification and Quantification

For protein identification, MS/MS data were searched using a local Mascot server (v2.6.2; Matrix Science, London, UK) against a database containing the sequences from all *B. subtilis* entries as found in SwissProt (version 2019_10, 4,298 sequences) and the corresponding 4,298 reverse sequences. The database was generated using MSDA software [23]. Spectra were searched with a mass tolerance of 10 ppm for MS and 0.07 Da for MS/MS data, allowing a maximum of one trypsin missed cleavage. Carbamidomethylation of cysteine residues and oxidation of methionine residues were specified as variable modifications. Identification results were imported into Proline v2.1 (www.profi-proteomics.fr/proline) for validation. Peptide Spectrum Matches (PSM) with pretty rank

equal to one and with a minimum sequence length of 7 were retained. False Discovery Rate was then optimized to be below 1% at PSM level using Mascot Adjusted E-value and below 1% at the protein level using the Mascot score. Peptide abundances, were extracted using a m/z tolerance of 10 ppm. Alignment of the LC-MS runs was performed using Loess smoothing. Cross Assignment was performed between all runs. Protein abundances were computed as the sum of all peptide abundances (normalized using the median). Peptides sharing peakels were discarded.

The mass spectrometry proteomics data have been deposited to the ProteomeXchange Consortium via the PRIDE partner repository [24], with the dataset identifier PXD055248 and 10.6019/PXD055248.

2.5.4. Data Analysis

For global analysis, proteins identified with a single peptide or detected at most in only one replicate were discarded. For analysis of protein abundances data, values were normalized to 10^9 total counts for all the samples and a 1 was imputed to missing data in order to avoid “dividing by 0” errors. Mann-Whitney U-test was then performed and proteins were considered to vary significantly between two conditions when U was ≤ 2 for 4 replicates or ≤ 1 for 3 replicates, which correspond to a P value inferior to 0.05. No quantitative change threshold value was applied.

Analysis of varying proteins or pathways was then performed manually with the help of the Subtiwiki database [2]. Another approach was to look at the different proteins regulated by a specific regulator. Data from the Subtiwiki database were used to build the interaction matrix, and the yED Graph Editor (Version 3.23.2 Powered by the yFiles Graph Visualization Library <http://www.yWorks.com>) was used for displaying the regulon networks with an organic layout. Only proteins detected by mass spectrometry at least in one conditions are represented plus in some cases the regulators. All the proteins varying significantly or nor are shown but using two shades of the same color. In many cases, proteins are regulated by more than one regulator, but for the simplicity of the representations we purposely dealt with one regulator at a time and not a complex network.

2.5.5. Principal Coordinates Analysis

The complete proteomic data table was analyzed by Principal Coordinates Analysis (PCoA, MDS), using the PAST software V4.03 [25]. The Gower distance was used for calculations. The first two axes of the Principal Coordinates Analysis were used as axis in the representation with eigenvalue scale and represent 68% of the total variance.

2.6. *ppGpp* assay

2.6.1. Crude Extract Preparation

Crude extracts were prepared from the frozen cells by resuspending them in the lysis mix: 600 μ L of Z-buffer 1x (60 mM Na_2HPO_4 , 40 mM NaH_2PO_4 , 10 mM KCl, 1 mM MgSO_4 , pH 7), 60 μ L of 1/50 Nuclease Benzonase solution (E-1014 from SIGMA), 300 μ L of Lysozyme 8 mg/mL and 2040 μ L of H_2O for a final volume of 3 mL. The cells were incubated at 37°C for 30 min and the supernatant corresponding to the crude extract was recovered after 2 min of a centrifugation at 13,000 rpm. Part of the crude extract was taken for total protein quantification using the Bradford assay and part for the *ppGpp* assay.

2.6.2. *ppGpp* Quantification

The *ppGpp* content was measured as previously described by Zheng et al. [26]. A 100% solution of trichloroacetic acid (TCA) was added to the supernatants in order to reach 10% of TCA in the final solution and the crude extracts were incubated at 4°C for 1h. Then the tubes were centrifuged and the supernatants recovered. A solution for the Fenton reaction was prepared and composed of 3 mL of acetate buffer (TpAc) 50 mM pH 3.6, 1.5 mL of FeCl_3 50 μ M and 3 mL of H_2O_2 1M (for a final volume of 7.5 mL). The ABTS (2,2'-Azino-bis(3-ethylbenzothiazoline-6-sulfonic acid) stock solution was prepared at 2.5 mM. Then, the TpAc (500 μ L), the ABTS solution (100 μ L), the supernatants (0,

100 or 200 μL) and H_2O (QSP 1mL) were mixed and incubated 30 min at 37°C . At the end the $\text{OD}_{414\text{ nm}}$ was measured for each condition. All experiments were performed in quadruplicate (four independent growth cultures).

2.7. Biofilm Quantification with Crystal Violet

After being incubated without shaking at 30°C for 48h, the planktonic bacteria were removed and the $\text{OD}_{600\text{ nm}}$ was measured. The sessile bacteria forming a pellicle biofilm were rinsed twice with 1mL of PBS. All liquid was carefully removed, cells were dried 10 min at room temperature and then, incubated with 1mL of 0.3% Crystal violet. After 10 min at room temperature, the Crystal violet solution was removed, the cells were rinsed with 2mL of PBS, and dried during 30 min. Then, 4mL of 95% ethanol was added in each well. After 10 min, the solution was removed, and diluted as required to be measured at 595 nm.

2.8. Sporulation

All of the cells contained in each well were pelleted and frozen at -20°C as described before. The pellets were resuspended in 20 mM phosphate buffer (pH 7.4) to an $\text{OD}_{600\text{ nm}}$ approximately of 1. Half of the sample was incubated at 80°C for 10 min and appropriate dilutions were plated on LB plates. CFU were counted after overnight incubation at 37°C . In parallel, the protein concentration was assayed using a Bradford assay [27]. The results were expressed as number of spores normalized by the protein quantity. All experiments were performed in triplicate (three independent growth cultures) and with at least two technical replicates.

Quantification of remaining spores after preparation of the crude extract: for this, we looked indirectly at the proportion of spores able to germinate after being put in contact with the lysis buffer. After the incubation in the CTAC-Urea-phosphate buffer lysis buffer as described above, 10% of the crude extract was assayed using a Bradford assay. The remaining 90% were centrifuged 10 min at 13 000 rpm. The pellets were resuspended in 1 mL of PBS and serial dilution from 10^0 to 10^{-6} were plated on LB agar.

3. Results

3.1. Cerium and Silicon Oxide NP Aggregation States Are Identical in All Media

NPs were characterized with DLS in term of size and for their potential aggregation in the culture medium. As shown in Figure 1, the vast majority of cerium (around 70%) is encountered in particles in the range 100-1000 nm with an average around 300 nm in LB medium. There is a slight decrease in the proportion of particles bigger than 100 nm in the LB medium compared to water as the organic matter in the LB may decrease aggregation. The variations in size between the different media (water, LB medium and supernatant from *B. subtilis* culture in LB) are not significant. Similar results are obtained for silica particles (data not shown).

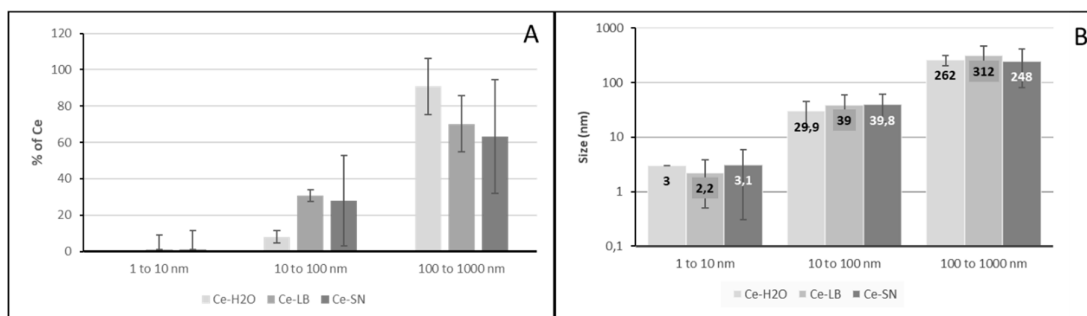


Figure 1. DLS characterization of cerium oxide nanoparticles. Panel A: repartition of cerium between various NP size ranges in function of the medium (water, LB broth, or culture supernatant (SN)).

Panel B: average radius of the NP in function of the medium: water (light grey), LB broth (medium grey) or culture supernatant (SN) (dark grey). Error bars represent standard error of the mean (sem).

3.2. Choice of the NP Doses to Be Studied

To decipher the impact of the growth conditions, biofilm and swarming, on bacterial physiological response, an identical dose of nanoparticles was applied in both conditions. We therefore decided, based on data in the literature, to assay a high dose similar to what has been described for eg. by Pop et al. in 2020 as already triggering some inhibitory effects for their CeO₂ NPs [28], and a lower dose i.e., 100 times lower. We decided as well to study the same concentrations for both Ce and Si oxide NPs that is 10⁻⁴ and 10⁻² mg/mL.

3.3. Differential Shotgun Proteomic Highlights Significant Variations between the Different Growth Conditions (Swarming and Pellicle Biofilm with or without Nanoparticles)

3.3.1. Sample Preparation Verification: No Significant Viable Spores Left in the Crude Extract

B. subtilis being able to sporulate and the spores being very resistant to various detergents and lysis conditions, we decide to check that the buffer used based on urea and CTAC (see details in Materials and Methods) was able to break down these structures and ensure that all proteins, including those of spores, were analyzed. For this, the quantity of spores remaining after preparation of the crude extracts was measured. No detectable viable spores were present in the crude extract from the cells grown in biofilm condition. Only an average of 44 spores remained in the solubilized extracts compare to an average of 2.7 10⁴ spores in the pellets of swarming cells which can be considered as negligible. Therefore, in both growth conditions, all or almost all the spores contained in the biofilms have been lysed.

3.3.2. Shotgun Global Results Show a Variable Number of Significantly Varying Proteins between the Different Conditions

Proteomic analyses were performed for two doses of Ce oxide or silica NP (Ce^H: 10⁻² mg/mL and Ce^L: 10⁻⁴ mg/mL; Si^H: 10⁻² mg/mL and Si^L: 10⁻⁴ mg/mL) in two growth conditions (swarming and pellicle biofilm) during 48h. A set was also obtained in pellicle biofilm conditions after 72h by incubating with 1/3rd of the doses and changing the medium every 24h. Experiments were performed in quadruplicate except for one condition for which the analysis failed (Ce^L, biofilm 48h). The shotgun proteomic analysis was able to detect and quantify 1544 proteins (Table S1). We then observed that three proteins, i.e., Cell wall-associated protease (wprA gene, secreted quality control protease, extracellular, cell wall bound), Bacillopeptidase F (bpr gene, extracellular) and Flagellin (hag gene, extracellular, major component of the secretome, membrane bound) could represent up to 40, 20 and 43 % of the total proteins (Table S2). Moreover, there is a great variability between the replicates and consequently, the variations are such as they biased the calculation of other proteins variations. Therefore, the data have been reanalyzed by removing these three proteins from the Mascot interrogation database. After cleaning for proteins identified with only one peptide, or detected at most once per condition quadruplicate, a complete list of 1272 proteins (Table S3) was obtained. Proteins modulated by the difference in growth conditions or exposure to NPs were selected on the basis of a Mann-Whitney U test ≤ 2 (or ≤ 1 in the case of only 3 replicates), which corresponds to $p \leq 0.05$. This resulted in the selection of a variable number of modulated proteins depending on the conditions compared as summarized in Table 1. For the remaining of this paper, the analyses will first focus on the comparison at 48 h of the pellicle biofilm vs swarming and secondly on Ce oxide NP toxicity observed in the two growth conditions at 48h.

Table 1. Number of modulated proteins between various conditions.

Number of modulated proteins	Control pellicle biofilm 48h vs swarming					
down U≤2	239					
up U≤2	348					
down U≥2	399					
up U≥2	281					
	Swarming Ce ^H vs ctrl	Swarming Ce ^L vs ctrl	Biofilm 48h Ce ^H vs ctrl	Biofilm 48h Ce ^L vs ctrl	Biofilm 72h Ce ^H vs ctrl	Biofilm 72h Ce ^L vs ctrl
down U≤2	321	8	74	141	18	7
up U≤2	31	4	102	58	7	7
down U≥2	735	744	697	601	853	631
up U≥2	165	504	386	460	385	620
	Swarming Si ^H vs ctrl	Swarming Si ^L vs ctrl	Biofilm 48h Si ^H vs ctrl	Biofilm 48h Si ^L vs ctrl	Biofilm 72h Si ^H vs ctrl	Biofilm 72h Si ^L vs ctrl
down U≤2	16	10	87	78	10	28
up U≤2	11	5	66	59	51	130
down U≥2	845	762	640	599	627	665
up U≥2	388	472	465	521	576	442

3.3.3. Cells under Swarming and Pellicle Biofilm Growth Conditions Differ Widely in Their Proteomes, Highlighting Important Divergent Physiological Adaptations

Pathways Analyses

As shown in Table S4, in the pellicle biofilm a huge number of ribosomal proteins, transporters (mainly for acquisition and synthesis of amino acids), proteins of the central carbon metabolism (TCA, gluconeogenesis), utilization of various carbon sources... are up-regulated compared to swarming conditions. Tables S5, mainly based on Subtiwiki data [2], highlights some of these aspects like Table S5A for core carbon metabolism.

As shown in Table S5B proteins implicated in sporulation are less abundant in biofilm except maybe for the initiation of sporulation. Proteins implicated in germination are also rather down-regulated. On the opposite, proteins implicated in biofilm formation, in motility are globally more abundant in pellicle biofilm vs swarming. The respiratory chain including ATPase are rather up regulated (Table S5C). As shown in Table S5D, in the pellicle biofilm, proteins for amino acid acquisition or synthesis are globally up regulated (except for arginine), and proteins like P71035, (urease beta subunit, utilization of urea as alternative nitrogen source) or P19406 and P19405 (alkaline phosphatases, acquisition of phosphate upon phosphate starvation) are less expressed. This tends to indicate that in the biofilm the bacteria are not lacking of nutrients. This is also reflected by the lower expression of extracellular feeding proteases (P04189, P39790, P29141, see Table S5E). Concerning metal, in the biofilm proteins for Mn or Fe acquisition are up regulated as well as iron-sulfur cluster synthesis by SUF proteins whereas heme biosynthesis pathway seems to be rather down regulated (Table S5F). Looking at lipids metabolism, one can see that it is differently regulated between the two modes of growth with a somehow increase of synthesis but mostly a decrease of fatty acid degradation (Table S5G). At last, it is also possible to see a high impact on different types of stresses. As illustrated in Table S5H, in term of resistance to oxidative stress many proteins are expressed at a higher level in the pellicle biofilm such as P80239 and P42974 (alkyl hydroperoxide reductase, small and large subunits), P26901 and P42234 (catalases), O34777 (regulation of ohrA expression in response to organic peroxides), P71086 (transcriptional repressor of the peroxide regulon, sensor of the intracellular Fe/Mn ratio, regulation of the response to peroxide), Q796Y8 (similar to thioredoxin-

dependent hydroperoxide peroxidase), and P52035 (similar to glutathione peroxidase). On the other hand, O35023 (superoxide dismutase, detoxification of oxygen radicals) is down regulated.

Regulon Analyses

Another way to study the general response is to consider the regulators and the proteins they regulate (regulon). Using the database of Subtiwiki [2], a series of global regulators such as the sigma factors or the stringent response as well as a few more specific ones such as Spo0A (initiation of sporulation), ComK (regulation of genetic competence), FadR (repressor of fatty acid degradation) have been investigated to see if a regulon is activated or not, knowing that some of the regulated proteins can also be modulated by other regulators, sometimes in different ways, and influence the results. This analysis clearly shows that there is less stringent response in biofilm than in swarming (Figure S1). We can also see that proteins implicated in branched chain amino acid utilization, controlled in part by BkdR, are up regulated, which is consistent as branched chain amino acid limitation is one of the main triggering factor of stringent response. For sporulation, sigma factors for late stages seems to be activated for swarming (less expression for biofilm) but a little bit less for earlier stages (Figure S2-S6). Studies on the two regulators of competence ComA and ComK are not conclusive (Figure S7), and the study of SigD regulon tends to show a slight stimulation in term of motility in biofilm compared to swarming (Figure S8). A decrease in proteins implicated in fatty acid degradation is also clearly visible when analyzing FadR regulon (Figure S9). Concerning stress, the SigB and PerR regulons are not in the same state between the two modes of biofilm, nor are the proteins implicated in metal homeostasis (mainly iron and manganese) at the same basal level (Figure S10-S11). The difference is also visible in term of DNA repair (Figure S12).

Pathway and regulon analyses all lead to the same conclusion considering the metabolic state of the cell, indicating that in average the bacteria are metabolically more active in the pellicle biofilm conditions than in the swarming growth conditions.

Validation Experiments

Several experiments were set-up to confirm these results.

- ppGpp measurement: the stringent response is increased in swarming growth conditions

The activation of the stringent response was analyzed by measuring the alarmone ppGpp as described in Material and methods. Figure 2 clearly shows that cells growing in swarming condition contain more ppGpp (lower OD_{414 nm}) than in pellicle biofilm growth conditions, which correlates with a higher stringent response.

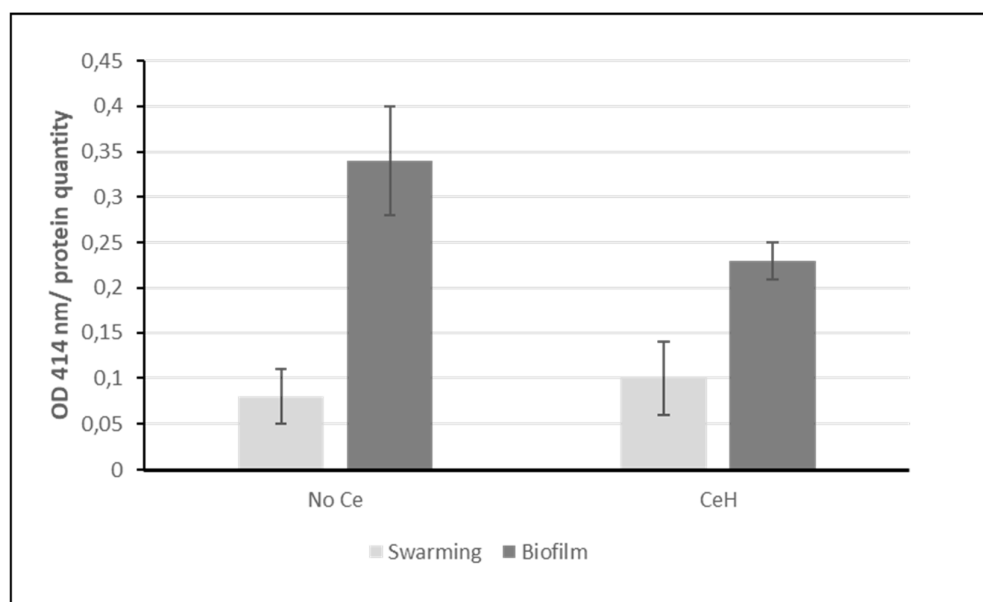


Figure 2. ppGpp assay. ppGpp concentration is inversely correlated to the OD measured at 414 nm. The OD is normalized to the protein quantity used in the assay. Error bars represent standard error of the mean (sem). Light grey: swarming conditions; dark grey: pellicle biofilm conditions.

- Sporulation is increased in swarming growth conditions

Due to the difficulty of dissociating all the cells from the biofilm matrix without heating and count them, the number of spores was normalized to the protein quantity. As shown in Figure 3, more spores are present in swarming than in biofilm mode in perfect match with proteomic analyses.

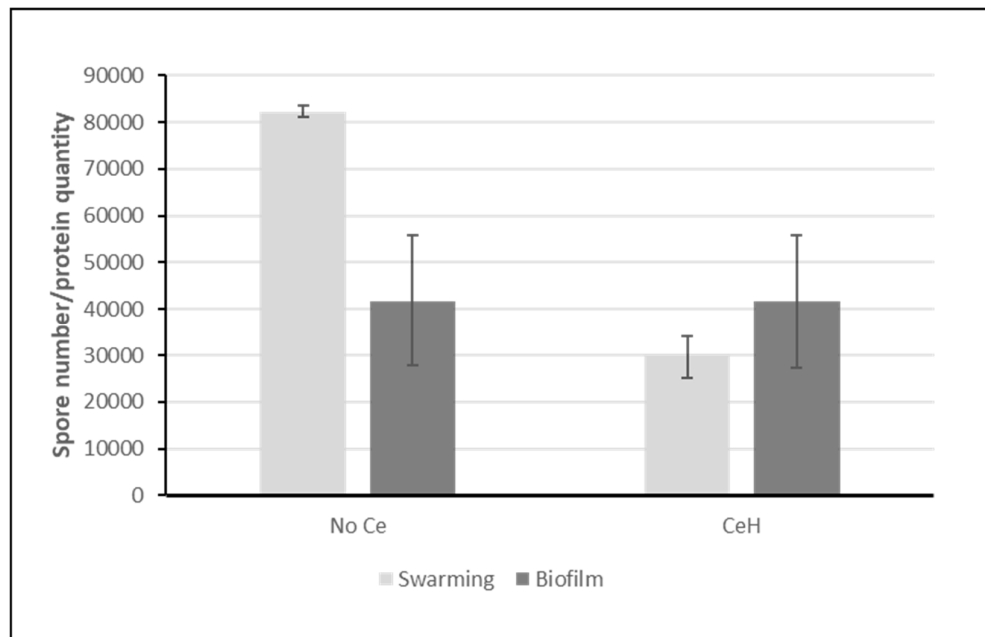


Figure 3. sporulation. Bars represent the number of spores normalized by the protein quantity used in the assay. Error bars represent standard error of the mean (sem). Light grey: swarming conditions; dark grey: pellicle biofilm conditions.

As a result we can conclude that after 48 h without NPs, the bacterial populations end up in a quite different state with on average for biofilm more metabolically active cells but with more oxidative stress, and for swarming more nutrient stressed cells, less metabolically active but in a physiological state (more spores) that is a way to fight stress.

3.3.4. Ceria Nanoparticles Exacerbate Cellular Stress Responses Particularly in Swarming Growth Conditions

Principal Coordinates Analysis

A first global investigation by principal coordinates analysis was performed on the data obtained at 48 h on the two types of biofilm with Ce and Si oxide NPs. Figure 4 clearly shows that the differences between the two modes of culture are greater than those between the NP-exposed cells and their non-exposed control. The analysis also show more reproducibility between replicates in the pellicle biofilm conditions than in the swarming conditions.

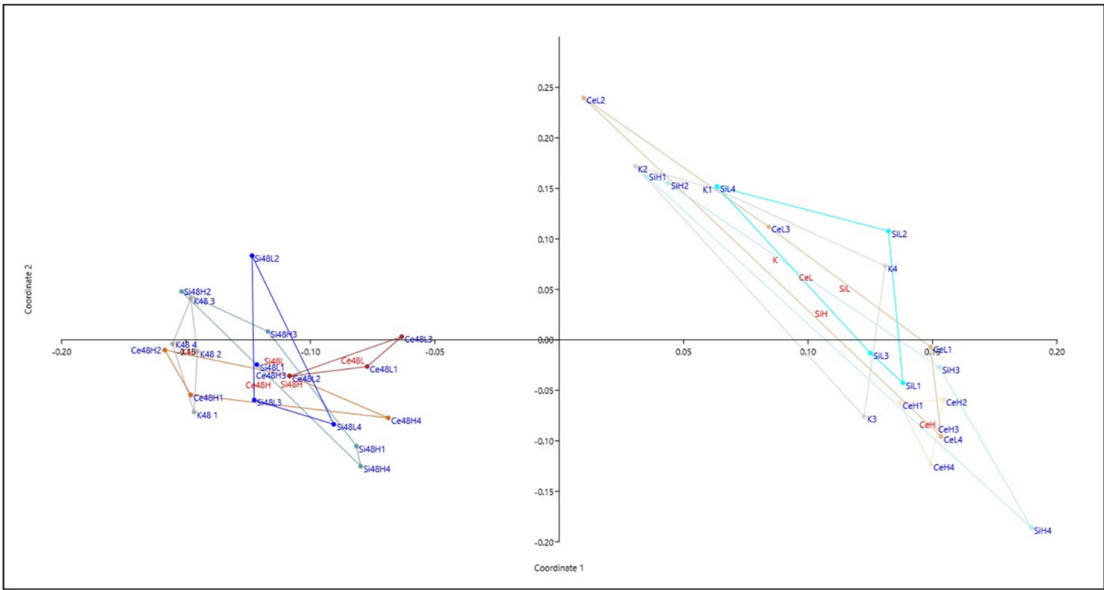


Figure 4. principal coordinates analysis The Gower distance was used for calculations. The first two axes of the principal coordinates analysis were used as axis in the representation with eigenvalue scale and represent 68% of the total variance. In red, group label and in blue replicates with their number. H and L for high and low dose, respectively (10 µg/mL or 0.1 µg/mL). On the left, names with 48 indicates pellicle biofilm samples at 48h and otherwise (on the right) names are associated with swarming samples. K stands for control without nanoparticles, Si for nanosilica and Ce nanoceria exposed samples.

Comparative Analysis with Cerium Oxide NPs

As seen in Table 1, there is almost no significantly modulated proteins when bacteria are exposed to the lower concentration of Ce oxide NPs in swarming conditions whereas at the higher concentration more than 320 proteins are down-regulated and 31 up-regulated (Table S6). In pellicle biofilm, around 190 proteins are significantly modulated (up or down) (176 for Ce^H vs control and 199 for Ce^L vs control) (Table S7). As shown in Figure 5 for Ce^H, few proteins are significantly regulated in the same way in both culture conditions. For example, YisY (spore coat protein) and CgeC (implicated in the maturation of the outermost layer of the spore) are both up-regulated. On the other hand, only 4 proteins are significantly regulated in the opposite direction (including YeaA and YdjL, two poorly characterized cell envelope stress proteins implicated in sporulation). It is nonetheless noteworthy that about 2/3 of the proteins that vary significantly in one direction have a ratio change in the same direction in the other growth condition, even if not always statistically significant, suggesting that the response is not so drastically different in the two modes of culture.

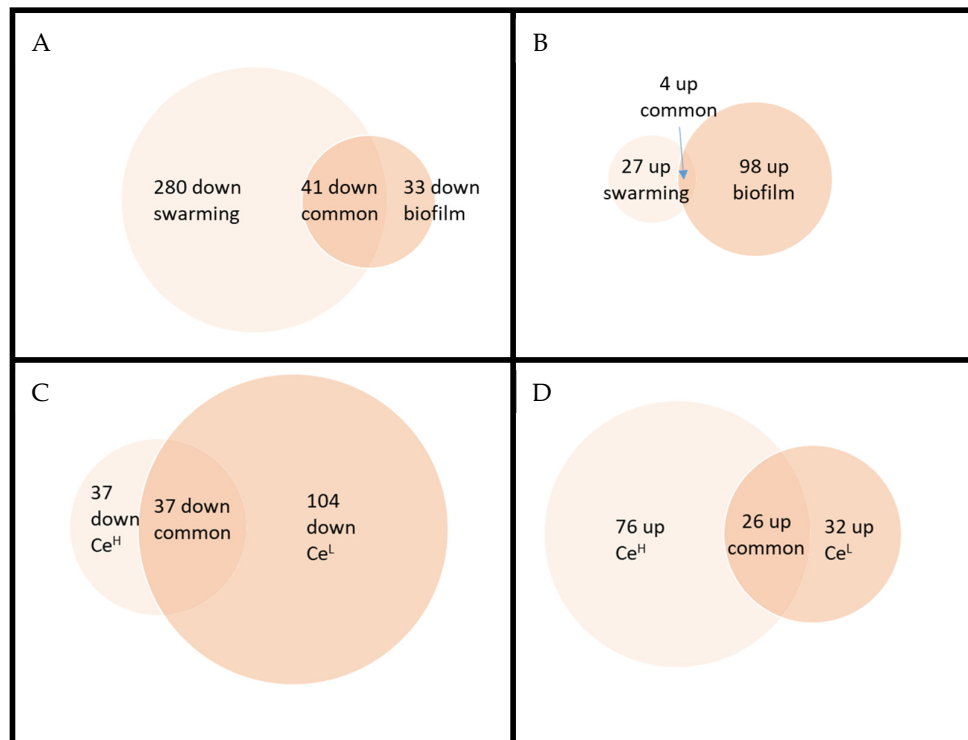


Figure 5. Venn diagrams for comparing the effects of a high dose of nanoceria between the two mode of growth conditions (Panel A and B) and the effects of two doses of nanoceria on bacteria grown in pellicle biofilm conditions.(Panel C and D). Panels A and C deals with down regulated proteins and panel B and D with up-regulated ones.

Comparing the responses of bacteria exposed to the two doses of Ce in pellicle biofilm conditions, only around 1/3 vary significantly in the same way (none in the opposite direction) but once again in the majority of the cases proteins vary in the same direction but with an uncertainty above the fixed threshold ($P < 0.05$).

In swarming, all the proteins varying significantly in the carbon core metabolism are downregulated in the presence of Ce (Table S8A) and for example, the catabolic repressor CcpA is clearly activated (Figure S13) whereas in biofilm (Table S9A), this is more divided. Besides, down-regulated proteins tend to be less down regulated in biofilm than in swarming (eg. P37869, Enolase ratio 0.5 in swarming vs 0.75 in biofilm; P54418, Phosphoenolpyruvate carboxykinase 0.38 vs 0.74; P21882 Pyruvate dehydrogenase subunit beta 0.45 vs 0.83; P21880 Dihydrolipoyl dehydrogenase 0.46 vs 0.78). In fact, the general tendency for Ce effect in swarming conditions, is the opposite of the previous comparison Biofilm vs swarming suggesting that Ce “aggravates or reinforces” the metabolic scheme set up by *B. subtilis* in swarming conditions. The same conclusion also stands for nitrogen assimilation (see for eg. *tnrA* regulator, Figure S14). We can notice as well that the stringent response is highly activated in the presence of Ce (Figure S1). Some coat proteins are largely increased like P07788 (CotA, laccase), O06734 (YisY, spore coat protein, similar to chloride peroxidase) or P42091 (maturation of the outermost layer of the spore) that correspond primarily to the protection of the spore. On the other hand, looking at the regulons implicated in sporulation, the response seems to be more mitigated. For example, SigG, H and K dependent transcription seems rather down regulated (Figure S2, S5). One can also note that proteins regulated by FadR are down regulated (Figure S9) yet the *fadNAE* operon encoding the β -oxidation enzymes is induced at the onset of sporulation [29]. Heme biosynthesis and iron transporters are also even more down regulated in the presence of Ce (Table S8F). At last, the down regulation of the SigB regulon suggests less oxidative stress (Figure S10). An effect on two others stress regulators (*ctsR* (general stress protein) and *spx* (cell envelope stress protein)) is also visible on Figures S15 and S16. In pellicle biofilm, the response

of *B. subtilis* to Ce exposure is much more ambivalent. A slight increase of proteins implicated in sporulation (Table S9B) and a decrease of those implicated in amino acid acquisition (Table S9D) can be nonetheless observed. Even if only a few proteins are down-regulated in a statistically significant way, the number of proteins involved in the stringent response, varying with a ratio inferior to 1 lets suggest (light blue in Figure S1) a slight increase of this response. SigK regulon (Figure S5) also suggests a slight increase in late sporulation genes.

Validation Experiments

- Stringent response in pellicle biofilm is increased upon nanoceria exposure

The ppGpp assay (Figure 2) shows that in pellicle biofilm conditions the alarmone for stringent response is indeed increased confirming the tendency observed on the regulon scheme. For swarming conditions, the change in the presence of Ce is not significant. Maybe the level of ppGpp has already reached its maximum without Ce or its increase may have occurred earlier with Ce and started to decrease at 48 h whereas the effect on proteins may still be visible.

- Sporulation response to nanoceria exposure depends on the growth conditions

Concerning sporulation, no difference is observed for biofilm growing conditions and a decrease is seen in swarming ones in agreement with the trend suggested by regulon analysis.

- Nanoceria promote biofilm formation

The effect of Ce exposure on biofilm formation was investigated by measuring the planktonic cells that remain in the culture medium and quantifying the biofilm. It is clear that less bacteria are present in solution in the presence of Ce and a slight increase is visible for the biofilm as measured by the Crystal violet (Figure 6).

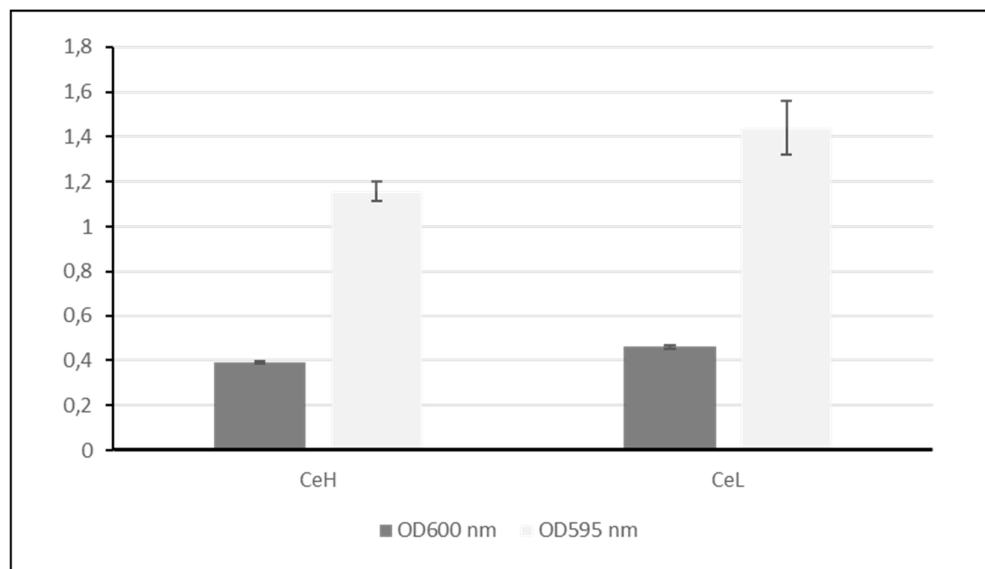


Figure 6. biofilm formation. Dark grey bars represent the planktonic cells as evaluated by the measure of the OD at 600 nm. Light grey bars represent the biofilm as estimated by the Crystal violet staining method and reading of the OD at 595 nm. In both cases, values are normalized by the values of the controls. Error bars represent standard error of the mean (sem).

In summary, in pellicle biofilm growth conditions, Ce effect is moderate but a decrease of the planktonic cells, and the premises of an increase in the stringent response and sporulation have clearly been observed. In swarming growth condition, cells were already relatively stressed and Ce has a rather additive effect except in terms of sporulation.

4. Discussion

Proteomic is a Powerful Technique to Analyse Proteome Complexity and Detect Faint Effects

This study has clearly shown that proteomics is a powerful and complementary approach to the microbiological assays in order to determine the global physiological state of a population of bacterial cells and to analyse the complexity of the genome in response to some small environmental changes (two biofilms growth conditions). It is also highly efficient to analyze the effect of toxicants. Indeed, proteomics can detect effects at doses for which the microorganism is still able to compensate. Some macroscopic phenotypes show no significant difference but the proteomic analysis allows deciphering at a molecular level the consequence of a toxic element in the environment. For example, even if a change in spore frequency is not statistically significant after Ce exposure at 10^{-2} mg/mL, the level of some protein associated with sporulation starts to increase.

Regulon Analysis Is Complimentary to Pathways Analysis and Compensate Partially the Lack of Proteoforms Analysis

In addition to analyzing the pathways in which modulated proteins are implicated, one can note the power of analyzing regulons. Indeed, for many proteins and especially regulators, their functions depend not only on their protein level but also on post-translational modifications such as phosphorylation or the presence of non-protein “regulators” (e.g., metabolites, metallic ions...). The regulon analysis allows to some extent (for regulators) to compensate for the fact that proteoforms were not specifically investigated in our proteomic studies but only canonical proteins as encountered in the SwissProt database. For example, in the biofilm vs swarming analysis, PerR is more abundant but the proteins it is supposed to repress are mainly up-regulated suggesting that iron is not bound to the protein and that PerR is not active.

Nanoceria Toxicity Is Highly Dependent on the Growth Conditions

Several studies have looked especially at Ce oxide NP toxicity in term of bactericidal action but mainly by well or disk diffusion methods or just growth inhibition [14,28,30]. They did not analyze any further the impacted pathways or functions. Pelletier et al. showed that the toxicity of nanoceria is highly dependent on the bacteria, concentration and size of the NPs, type of medium and pH [16]. They used transcriptomic on *Escherichia coli* and found only a handful of altered genes mainly implicated in sulfur metabolism or in the respiratory chain, and concluded that the response was complex and probably implied a moderate general stress response. In our study, we show that the response is also highly dependent on the growth conditions.

Nanoceria Alter Antioxidant Enzyme Level and the General Stringent Response

Most NPs like AgO, ZnO, TiO₂ interfere with stress resistance [31], or kill the cells via ROS production [11]. CeO₂ NPs possess very special redox properties that confer them antioxidant properties in some conditions hence their use to fight some diseases associated with oxidative stress. However, these properties are in fact highly dependent on the pH, coating of the particles [17]... In our case, in swarming conditions, SigB and PerR regulons are down regulated which could indeed correspond to a decrease in oxidative stress in the presence of nanoceria. In biofilm compare to swarming, the basal level of antioxidant enzymes like catalase (KatA, KatE), alkyl hydroperoxide reductase (Ahp), or proteins similar to thioredoxin-dependent hydroperoxide peroxidase (YgaF), and glutathione peroxidase (BsaA) is higher so the beneficial effect of the NPs may be less important. Moreover, biofilm is supposed to represent a physical barrier against different molecules but may also prevent their beneficial effects.

Concerning the fact that the stringent response is even more activated in the presence of Ce NPs in the swarming condition, one hypothesis could be that some essential nutrients that are already limiting are now also binding to the particles. Indeed, many NPs are able to bind proteins, phosphate...Ce being a hard metal is going to bind avidly phosphate (including phosphate in DNA).

One can note that for example, PhoB implicated in Phosphate acquisition upon starvation is increased in the presence of nanoceria.

In their study, Krishnamoorthy et al. showed that Ce Oxide NPs altered membrane integrity [32]. However, contrary to our biofilm conditions, they used liquid cultures. As they do not specify if the multi-well culture plates used for their experiment are agitated or not, it remains possible that the observed effect be linked to a mechanical effect of the particle per se under shaking.

5. Conclusions

Many toxicological studies on bacteria are conducted using liquid cultures, which do not accurately reflect environmental conditions. In this study, we analyzed the effect of NPs in two types of biofilms supposed to be more representative of the natural growth conditions. Surprisingly, proteomic analysis showed both similar tendencies, but also notable differences between these two modes of culture. This highlights the importance of studying various growth conditions to closely mimic the real environment. In the future, it would be valuable to compare the effects of Ce NPs added during versus after biofilm formation.

Supplementary Materials: The following supporting information can be downloaded at: www.mdpi.com/xxx/s1, Table S1: proteomic results using complete *Bacillus subtilis* protein database. Table S2: percentage of the total abundance represented by each of the three majors extracellular proteins. Table S3: proteomic results using *Bacillus subtilis* protein database without P54423, P16397 and P02968. Table S4: proteins significantly regulated between pellicle biofilm at 48h and swarming. Table S5: proteins altered between pellicle biofilm and swarming, and classified by pathways. Table S6: proteins significantly regulated between cerium and control in swarming conditions. Table S7: proteins significantly regulated between cerium and control in pellicle biofilm conditions after 48h. Table S8: proteins altered in swarming conditions after exposure to Ce^{III}, and classified by pathways. Table S9: proteins altered in pellicle biofilm conditions after exposure to Ce^{III}, and classified by pathways. Figure S1: stringent response and BkdR. Figure S2: sporulation (SigF and SigH). Figure S3: sporulation (Spo0A, spoIID and SpoVT). Figure S4: sporulation (SigE). Figure S5: sporulation (SigG and SigK). Figure S6: sporulation (GerE, GerR and SdpR). Figure S7: competence (ComA and ComK). Figure S8: motility (SigD). Figure S9: fatty acid degradation (FadR). Figure S10: general stress response (SigB). Figure S11: metal homeostasis (MntR, Fur and perR). Figure S12: DNA repair (LexA and AdaA). Figure S13: CcpA. Figure S14: nitrogen assimilation (TnrA). Figure S15: stress protein (CtsR). Figure S16: cell envelope stress protein (Spx).

Author Contributions: conceptualization, C.L., E.D., T.R., H.D. and S.C.; methodology, C.L., E.D. and H.D.; validation, C.L., E.D., S.L. and H.D.; formal analysis, C.L., E.D. and H.D.; investigation, S.L. and H.D.; data curation, C.L., E.D. and H.D.; writing—original draft preparation, E.D.; writing—review and editing, C.L., E.D., T.R., H.D. and S.C.; visualization, C.L. and E.D.; project administration, C.L.; funding acquisition, T.R. and S.C. All authors have read and agreed to the published version of the manuscript.

Funding: This work was supported by the CNRS, the University of Grenoble Alpes, the University of Strasbourg, and the French Proteomic Infrastructure (ProFI; ANR-10-INBS-08-03).

Data Availability Statement: The mass spectrometry proteomics data have been deposited to the ProteomeXchange Consortium via the PRIDE partner repository [24], with the dataset identifier PXD055248 and 10.6019/PXD055248. Other data will be freely available on demand to the corresponding authors.

Conflicts of Interest: The authors declare no conflicts of interest.

References

1. Yuan C.;Ji X.;Zhang Y.;Liu X.;Ding L.;Li J.;Ren S.;Liu F.;Chen Z.;Zhang L., et al. Important role of *Bacillus subtilis* as a probiotic and vaccine carrier in animal health maintenance. *World J Microbiol Biotechnol.* **2024**, *40*, 268; doi: 10.1007/s11274-024-04065-0.
2. Pedreira T.;Elfmann C.; Stulke J. The current state of SubtiWiki, the database for the model organism *Bacillus subtilis*. *Nucleic Acids Res.* **2022**, *50*, D875–D882; doi: 10.1093/nar/gkab943.
3. Verstraeten N.;Braeken K.;Debkumari B.;Fauvart M.;Fransaer J.;Vermant J.; Michiels J. Living on a surface: swarming and biofilm formation. *Trends Microbiol.* **2008**, *16*, 496–506; doi: 10.1016/j.tim.2008.07.004.
4. Kearns D.B.; Losick R. Swarming motility in undomesticated *Bacillus subtilis*. *Molecular Microbiology.* **2003**, *49*, 581–590; doi: 10.1046/j.1365-2958.2003.03584.x.

5. Dergham Y.; Sanchez-Vizueté P.; Le Coq D.; Deschamps J.; Bridier A.; Hamze K.; Briand R. Comparison of the Genetic Features Involved in *Bacillus subtilis* Biofilm Formation Using Multi-Culturing Approaches. *Microorganisms*. **2021**, *9*, 633; doi: 10.3390/microorganisms9030633.
6. Newton R.; Amstutz J.; Patrick J.E. Biofilm formation by *Bacillus subtilis* is altered in the presence of pesticides. *Access Microbiol*. **2020**, *2*, e000175; doi: 10.1099/acmi.0.000175.
7. Grobas I.; Bazzoli D.G.; Asally M. Biofilm and swarming emergent behaviours controlled through the aid of biophysical understanding and tools. *Biochem Soc T*. **2020**, *48*, 2903-2913; doi: 10.1042/Bst20200972.
8. Lemon K.P.; Earl A.M.; Vlamakis H.C.; Aguilar C.; Kolter R. Biofilm development with an emphasis on *Bacillus subtilis*. *Current topics in microbiology and immunology*. **2008**, *322*, 1-16; doi: 10.1007/978-3-540-75418-3_1.
9. Pisithkul T.; Schroeder J.W.; Trujillo E.A.; Yeesin P.; Stevenson D.M.; Chaiaamarit T.; Coon J.J.; Wang J.D.; Amador-Noguez D. Metabolic Remodeling during Biofilm Development of *Bacillus subtilis*. *Mbio*. **2019**, *10*, e00623-00619; doi: 10.1128/mBio.00623-19.
10. Hoseinzadeh E.; Makhdoumi P.; Taha P.; Hossini H.; Stelling J.; Kamal M.A.; Ashraf G.M. A Review on Nano-Antimicrobials: Metal Nanoparticles, Methods and Mechanisms. *Curr Drug Metab*. **2017**, *18*, 120-128; doi: 10.2174/1389200217666161201111146.
11. Khezerlou A.; Alizadeh-Sani M.; Azizi-Lalabadi M.; Ehsani A. Nanoparticles and their antimicrobial properties against pathogens including bacteria, fungi, parasites and viruses. *Microb Pathogenesis*. **2018**, *123*, 505-526; doi: 10.1016/j.micpath.2018.08.008.
12. Siddiqi K.S.; Husen A.; Rao R.A.K. A review on biosynthesis of silver nanoparticles and their biocidal properties. *J Nanobiotechnol*. **2018**, *16*, ARTN 14; doi: 10.1186/s12951-018-0334-5.
13. Khalid N.B.; Sarwar M.; Rakha A.; Khalid A.M.; Munawar A.; Riaz A.; Rehman R.A.; Akhtar S. Medicinal honeycomb ceria nanoparticles' fabrication by using green synthesis method. *Appl Nanosci*. **2022**, *12*, 2933-2943; doi: 10.1007/s13204-022-02575-7.
14. Sehar S.; Naz I.; Rehman A.; Sun W.Y.; Alhewairini S.S.; Zahid M.N.; Younis A. Shape-controlled synthesis of cerium oxide nanoparticles for efficient dye photodegradation and antibacterial activities. *Appl Organomet Chem*. **2021**, *35*, e6069; doi: 10.1002/aoc.6069.
15. Adams L.K.; Lyon D.Y.; Alvarez P.J.J. Comparative eco-toxicity of nanoscale TiO₂, SiO₂, and ZnO water suspensions. *Water Res*. **2006**, *40*, 3527-3532; doi: 10.1016/j.watres.2006.08.004.
16. Pelletier D.A.; Suresh A.K.; Holton G.A.; McKeown C.K.; Wang W.; Gu B.H.; Mortensen N.P.; Allison D.P.; Joy D.C.; Allison M.R., et al. Effects of Engineered Cerium Oxide Nanoparticles on Bacterial Growth and Viability. *Appl Environ Microb*. **2010**, *76*, 7981-7989; doi: 10.1128/Aem.00650-10.
17. Lord M.S.; Berret J.F.; Singh S.; Vinu A.; Karakoti A.S. Redox Active Cerium Oxide Nanoparticles: Current Status and Burning Issues. *Small*. **2021**, *17*, e2102342; doi: 10.1002/smll.202102342.
18. Collin-Faure V.; Dalzon B.; Devic J.; Diemer H.; Cianfèrani S.; Rabilloud T. Does size matter? A proteomics-informed comparison of the effects of polystyrene beads of different sizes on macrophages. *Environ Sci-Nano*. **2022**, *9*, 2827-2840; doi: 10.1039/d2en00214k.
19. Muller L.; Fornecker L.; Chion M.; Van Dorsselaer A.; Cianfèrani S.; Rabilloud T.; Carapito C. Extended investigation of tube-gel sample preparation: a versatile and simple choice for high throughput quantitative proteomics. *Sci Rep-Uk*. **2018**, *8*, e8260; doi: 10.1038/s41598-018-26600-4.
20. Rabilloud T. Optimization of the cydex blue assay: A one-step colorimetric protein assay using cyclodextrins and compatible with detergents and reducers. *Plos One*. **2018**, *13*, e0195755; doi: 10.1371/journal.pone.0195755.
21. Lyubimova T.; Caglio S.; Gelfi C.; Righetti P.G.; Rabilloud T. Photopolymerization of Polyacrylamide Gels with Methylene-Blue. *Electrophoresis*. **1993**, *14*, 40-50; doi: 10.1002/elps.1150140108.
22. Quque M.; Brun C.; Villette C.; Sueur C.; Criscuolo F.; Heintz D.; Bertile F. Both age and social environment shape the phenotype of ant workers. *Sci Rep-Uk*. **2023**, *13*; doi: ARTN 186
23. 10.1038/s41598-022-26515-1.
24. Carapito C.; Burel A.; Guterl P.; Walter A.; Varrier F.; Bertile F.; Van Dorsselaer A. MSDA, a proteomics software suite for in-depth Mass Spectrometry Data Analysis using grid computing. *Proteomics*. **2014**, *14*, 1014-1019; doi: 10.1002/pmic.201300415.
25. Perez-Riverol Y. Proteomic repository data submission, dissemination, and reuse: key messages. *Expert Rev Proteomics*. **2022**, *19*, 297-310; doi: 10.1080/14789450.2022.2160324.
26. Hammer Ø.; Harper D.A.T.; Ryan P.D. PAST: Paleontological Statistics software package for education and data analysis. *Palaeontologia Electronica*. **2001**, *4*, e4.
27. Zheng L.L.; Huang C.Z. Selective and sensitive colorimetric detection of stringent alarmone ppGpp with Fenton-like reagent. *Analyst*. **2014**, *139*, 6284-6289; doi: 10.1039/c4an01632g.
28. Bradford M.M. A rapid and sensitive method for the quantitation of microgram quantities of protein utilizing the principle of protein-dye binding. *Anal Biochem*. **1976**, *72*, 248-254; doi: 10.1006/abio.1976.9999.
29. Pop O.L.; Mesaros A.; Vodnar D.C.; Suharoschi R.; Tăbăran F.; Măgeruşan L.; Tódor I.S.; Diaconeasa Z.; Balint A.; Ciontea L., et al. Cerium Oxide Nanoparticles and Their Efficient Antibacterial Application In Vitro

- against Gram-Positive and Gram-Negative Pathogens. *Nanomaterials*. **2020**, *10*, e1614; doi: 10.3390/nano10081614.
30. Fujita Y.;Matsuoka H.; Hirooka K. Regulation of fatty acid metabolism in bacteria. *Molecular Microbiology*. **2007**, *66*, 829-839; doi: 10.1111/j.1365-2958.2007.05947.x.
31. Kumar K.M.;Mahendhiran M.;Diaz M.C.;Hernandez-Como N.;Hernandez-Eligio A.;Torres-Torres G.;Godavarthi S.; Gomez L.M. Green synthesis of Ce rich CeO nanoparticles and its antimicrobial studies. *Mater Lett*. **2018**, *214*, 15-19; doi: 10.1016/j.matlet.2017.11.097.
32. Eymard-Vernain E.;Luche S.;© T.; Lelong C. ZnO and TiO₂ nanoparticles alter the ability of *Bacillus subtilis* to fight against a stress. *PLoS One*. **2020**, *15*, e0240510; doi: 10.1371/journal.pone.0240510.
33. Krishnamoorthy K.;Veerapandian M.;Zhang L.H.;Yun K.; Kim S.J. Surface chemistry of cerium oxide nanocubes: Toxicity against pathogenic bacteria and their mechanistic study. *J Ind Eng Chem*. **2014**, *20*, 3513-3517; doi: 10.1016/j.jiec.2013.12.043.

Disclaimer/Publisher's Note: The statements, opinions and data contained in all publications are solely those of the individual author(s) and contributor(s) and not of MDPI and/or the editor(s). MDPI and/or the editor(s) disclaim responsibility for any injury to people or property resulting from any ideas, methods, instructions or products referred to in the content.